AA528 Final Project
Transfer Orbit Design Proposal: Earth to Earth-Moon L4

Berit Syltebo

March 2023

1 Introduction

The goal of this project was to expand upon the Circular Restricted 3-Body Problem (CR3BP) discussed in this class and apply it to more complicated problems such as trajectory design. The theory behind equilateral libration points was the main point of intrigue when deciding how to best spend my time exploring the 3-body problem. In order to put together a complete analysis, proficiency in many new concepts were necessary including invariant manifold theory and machine learning techniques to optimize trajectories. Knowledge from this class could be applied when developing equations of motion and linearization for first approximations. There were definite shortfalls in my final output as much of my time was spent learning and attempting to reproduce simulations from complex models. Nevertheless, a design was proposed using a Hohmann transfer with relatively thorough investigation of L4 dynamics upon arrival. A final orbit around L4 is realized and important design parameters such as transfer timing and velocity correction costs are considered.

2 Investigation of transfer trajectories to and from the equilateral libration points L4 and L5 in the Earth-Moon system - Lucia R. Irrgang [2]

The motivation of this contribution was to utilize the advantageous location of the equilateral libration points for applications like deep-space communication by placing a satellite at one of these points. The paper bases its analysis around the Circular Restricted 3-Body Problem (CR3BP) and thus discusses the relevant dynamics from this approach (Section 2); this includes equilibrium points, linearization techniques, periodic solutions for libration point orbits, and invariant manifold theory. Some of these numerical methods and dynamics will be discussed more in-depth in the next section.

The third section of this paper explores motion about the equilateral libration points to determine periodic orbits using accurate models. The limitations of linear approximations for these orbits are thoroughly investigated to determine to what extent this simplified model is effective. This analysis is conducted for both short and long period orbits. It is clear from Figure 1 that the linear approximation breaks down as orbit trajectory gets further and further away from the libration point.

Due to the inaccuracies of linear approximations about these libration points, proceeding analyses only use nonlinear models. This allows for much more variability in periodic orbit size to suite a wider range of mission specifications. In fact, the short period orbit chosen as the final destination for the transfer is quite large in relation to the limitations of linearization so the increase in robustness was essential.

Rather than starting at Earth, the paper focuses on transfer to and from an L2 periodic orbit using the stable and unstable manifolds as ideal trajectories for the spacecraft. Section 4 covers planar transfers while Section 5 covers 3-dimensional. For the sake of this project, only planar will be summarized and considered. The derivation process highlighted was for a transfer from L4 to L2 following a stable manifold but also briefly explored how to get to L4 or L5 from L2 from an unstable manifold. An example of this trajectory can be found in Figure 2 where the magenta line represents the transfer starting at the magenta star. The transfer makes almost a full revolution about L2 before showing a significant difference between the

periodic orbit and the transfer.

3 Theory & Analysis Techniques

The potential energy of a spacecraft in a 3-body system can be computed using Equation 1

$$U = \frac{1}{2}(x^2 + y^2) + \frac{(1-\mu)}{d} + \frac{\mu}{r} \tag{1}$$

Evaluating the second partials of Equation 1 at the equilateral libration points yield the associated potential energy partials. The surprising simplification of these constants come from the geometric location of these libration points where, in non-dimensional units, they are located at $\left(\frac{1}{2} - \mu, \pm\frac{\sqrt{3}}{2}\right)$ with the positive y coordinate corresponding to L4.

$$\begin{aligned} U_{xx}|_{\vec{X}_{L_{4,5}}} &= \frac{3}{4} \\ U_{yy}|_{\vec{X}_{L_{4,5}}} &= \frac{9}{4} \\ U_{xy}|_{\vec{X}_{L_4}} &= \frac{3\sqrt{3}}{2}\left(\mu - \frac{1}{2}\right) \\ U_{xy}|_{\vec{X}_{L_5}} &= -\frac{3\sqrt{3}}{2}\left(\mu - \frac{1}{2}\right) \\ U_{zz}|_{\vec{X}_{L_{4,5}}} &= -1 \end{aligned} \tag{2}$$

The in-plane frequencies, as shown in Equation 3 are purely dependent upon the mass ratio, μ. Proceeding this expression reveal the derivation of constants s_1 and s_2 which define the magnitude of these in-plane frequencies and are used to compute the long and short period orbits, respectively.

$$\begin{aligned} \lambda_{1,2} &= \pm\sqrt{\frac{-1 + \sqrt{1 - 27\mu + 27\mu^2}}{2}} \\ \lambda_{3,4} &= \pm\sqrt{\frac{-1 - \sqrt{1 - 27\mu + 27\mu^2}}{2}} \end{aligned} \tag{3}$$

$$\lambda_{1,2} = \pm s_1 i \qquad \lambda_{3,4} = \pm s_2 i$$

The constants Γ_1 and Γ_2 are then used to obtain the initial velocity components in the xy-plane as seen in Equation 5. Of course, the initial position must first be chosen to obtain these conditions, or vice versa, to acquire a complete initial state for the dynamical system.

$$\Gamma_i = \left(\frac{s_i^2 + U_{xx}|_{\vec{X}_{L_i}}}{4s_i^2 + U_{xy}|_{\vec{X}_{L_i}}} \right)^2 \tag{4}$$

$$\begin{aligned} \dot{\xi}_0 &= \frac{1}{2}\left(U_{xy}|_{\vec{X}_{L_i}} \xi_0 + \frac{\eta_0}{\Gamma_i} \right) \\ \dot{\eta}_0 &= -\frac{1}{2}\left(\left(s_i^2 + U_{xx}|_{\vec{X}_{L_i}} \right) \xi_0 + U_{xy}|_{\vec{X}_{L_i}} \eta_0 \right) \end{aligned} \tag{5}$$

With the initial state fully realized, the 2-dimensional motion can be modelled using Equation 6 which is in non-dimensional time, τ.

$$\begin{aligned} \xi &= \xi_0 \cos(s_i \tau) + \frac{\dot{\xi}_0}{s_i} \sin(s_i \tau) \\ \eta &= \eta_0 \cos(s_i \tau) + \frac{\dot{\eta}_0}{s_i} \sin(s_i \tau) \end{aligned} \tag{6}$$

4 Verification of Contribution Work

4.1 L4 Periodic Orbits

Knowing that rough initial and final conditions are necessary before starting a transfer trajectory design, I started by reproducing the motion about L4 using a linear approximation. Section 3 reveals the derivation for these dynamics such that only the mass ratio, μ, is need to create a skeleton for the equations of motion. The in-plane frequencies are easily computed using Equation 3 such that s_1 and s_2 are found. These computed quantities are shown below:

$$s_1 = 0.29820789544347032$$

$$s_2 = 0.95450094347526815$$

The paper by Lucia R. Irrgang is somewhat misleading in it's derivation of the initial conditions to complete Equation 6. I attempted to use the suggested initial conditions for both long and short period orbits but wasn't able to recreate the results. I later realized that the initial conditions given were in dimensional units and Equation 6 needed velocity components in terms of non-dimensional time. Using the provided equations to derive the velocity from scratch, I obtained wildly different numbers from those provided but ended up matching the results in the paper. The table below shows the proper inputs for the equations of motion and how the velocity vector compares in dimensional units.

s_i	s_2 (short period)	s_1 (long period)
ξ_0 (km)	384.388174	384.388174
$\dot{\xi}_0$	243.59871675129397	243.59871675129397
$\dot{\eta}_0$	-319.2482263014549	-161.2369911985452
$\dot{\xi}_0$ (km/s)	$6.493012243087153\times10^{-4}$	$6.493012243087153\times10^{-4}$
$\dot{\eta}_0$ (km/s)	$-8.509362006775028\times10^{-4}$	$-4.297671260030953\times10^{-4}$

To simplify the computation of these periodic orbits, the initial position was chosen with a y-position equal to that of L4 (ie. $\eta_0 = 0$). The result is equivalent ξ_0 properties between the short and long period orbits. Variations in the initial condition properties only appear in $\dot{\eta}_0$. Also important to note is the precision in these measurements; while L4 is marginally stable, these orbits behave such that any perturbations will cause the spacecraft to follow a new orbit and not converge back to the original. To maintain a stable orbit, a control system would need to be implemented to either make continuous or periodic corrections.

Implementation of the equations of motion with the computed initial conditions can be found in Figure 3.

4.2 Hohmann Transfer Design

Since I promised to provide a transfer trajectory from Earth to L4, I used the rest of my limited time (much was lost to attempts at the multiple shooting method) designing a Hohmann transfer using my results from Section 4.1.

Before designing the transfer properties, it's important to take into account the assumptions that come with a 2-body solution. A very simple

model of the 3-body problem is using the method of patched conics which stitches together a series of 2-body problems. The thresholds between these 'patches' are defined by the sphere of influences of the dominant bodies in the system. When a spacecraft enters a new sphere of influence, the dynamics can then be modelled using purely using the gravitation of that body.

To apply the method of patched conics to the Earth-Moon system, the dynamics of a spacecraft can be approximated using the Moon's gravity alone if it falls within $\text{SOI}_{☾}$, and the Earth's gravitation if it doesn't. This produces a crude model but can be used as a good first approximation in a design process. Assuming the lunar orbit is circular, an elliptical orbit from Earth to L4 orbit can be easily computed. Low Earth Orbit (LEO) at 300km altitude was chosen as the starting position for the spacecraft to simplify computation. The resulting properties of the orbit shape are summarized below:

$$e = 0.9657$$

$$a = 194685 \text{ km}$$

$$T_{transfer} = 4.947 \text{ days}$$

Next, using the transfer time, the time of transfer initiation was determined. The Moon travels 65.192° during the transfer and knowing that L4 is 60° ahead of the Moon, the fist burn (from LEO to transfer) would need to occur when the Moon is 125.192° behind the projected apogee. This is reflected in the transfer orbit simulation found in Figure 4 which is depicted in the Earth-Centered Inertial frame (ECI).

It is clear based on the to-scale drawing above that the transfer never falls within the sphere of influence of the moon and thus the dynamics of the spacecraft can be modelled using Earth's gravitation alone based on the rules of patched conics.

The last step I took in my analysis was solving for the necessary velocity corrections associated with the chosen transfer. Since the correction to get into the L4 periodic orbit are so small, they were not considered in my analysis. However, due to sensitivity around these points, these corrections would not be negligible for a real mission. A summary of these calculations are found below:

$$
\begin{aligned}
v_{\text{LEO}} &= 7.726\text{km/s} \\
v_{\text{transfer,p}} &= 10.832\text{km/s} \\
\Delta v_1 &= 3.106\text{km/s}
\end{aligned}
$$

$$
\begin{aligned}
v_{\text{transfer,a}} &= 0.189\text{km/s} \\
v_{☾} &= 1.021\text{km/s} \\
\Delta v_2 &= 0.832\text{km/s}
\end{aligned}
$$

5 Contribution Assessment

The main contribution provides a detailed mathematical background for for the topics of interest. This is how I was able to obtain models for the periodic orbits around L4. The only issue I had with it was how their transfer trajectory was from L2 to L4 rather than Earth to L4 as the title implied. There seemed to be a lot more investigation of the L2 manifolds and halo orbits than how to get to and from the equilateral libration points in practical scenarios. There was no explanation (that I could find) for why they were only considering transit with one collinear point and what real life purpose that would serve. I think the multiple shooting method could still be used with an Earth to L4 transfer and would like to see out how that would work. Perhaps the research turned into something the author wasn't expecting and deviated from their initial motivations.

References

[1] He, X., Liang, Y., Xu, M., amp; Zheng, Y. (2020). Low-thrust transfer to the Earth-moon triangular libration point via Horseshoe Orbit. Acta Astronautica, 177, 111–121. https://doi.org/10.1016/j.actaastro.2020.07.014

[2] Irrgang, L. R. (2008). Investigation Of Transfer Trajectories To And From The Equilateral Libration Points L4 And L5 In The Earth-Moon System (thesis).

6 Appendix

6.1 Figures

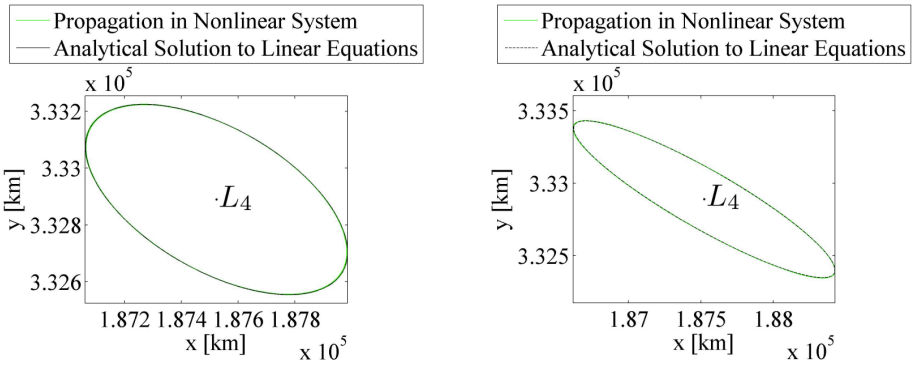

(a) Insertion distance ≈ 384km

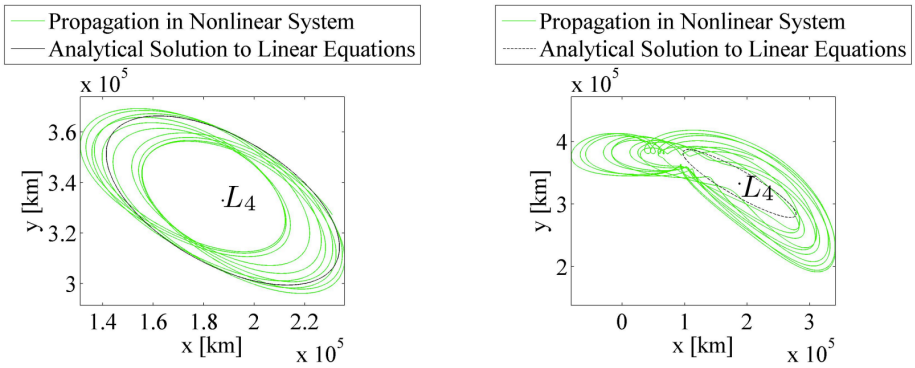

(b) Insertion distance ≈ 38400km

Figure 1: Comparison of linear and non-linear modelling for short and long period orbits about L4 with varying insertion distances

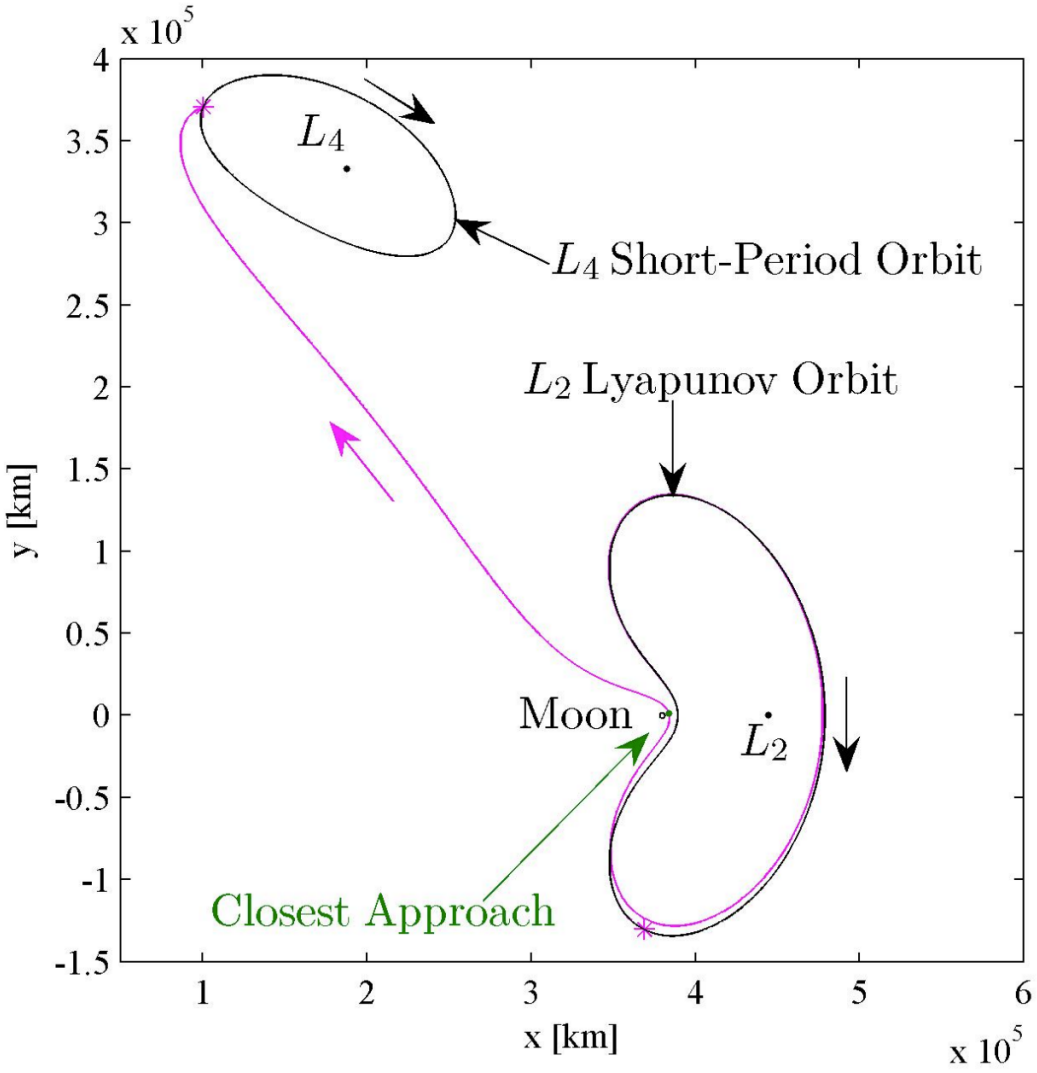

Figure 2: Example trajectory from L2 to L4 orbit

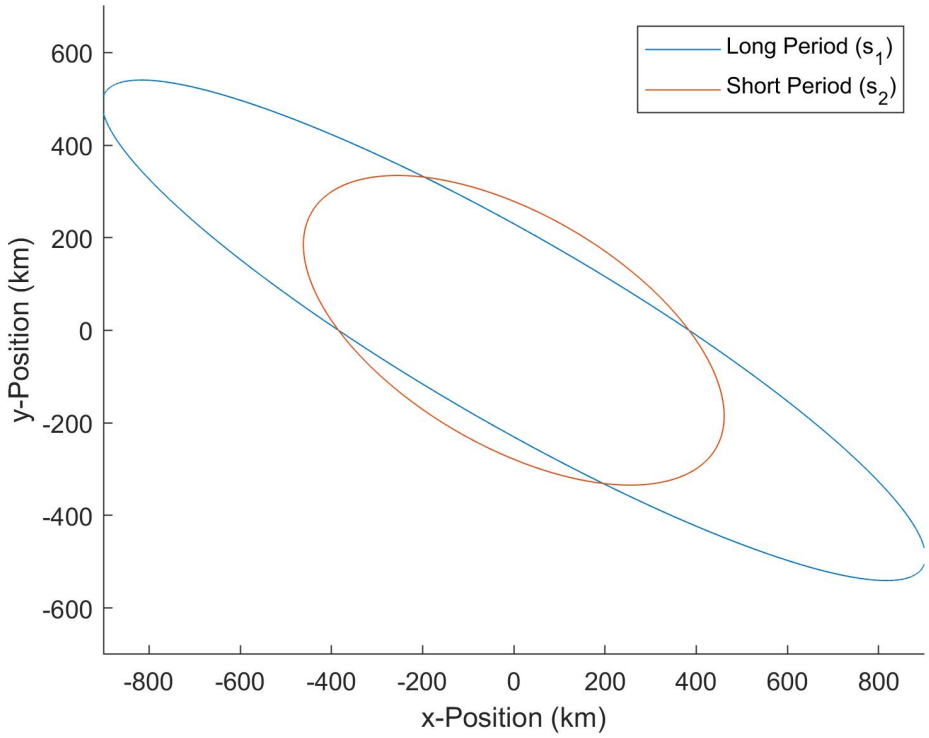

Figure 3: Simulation of short and long period orbits about L4 with an initial position of (384.388174,0)

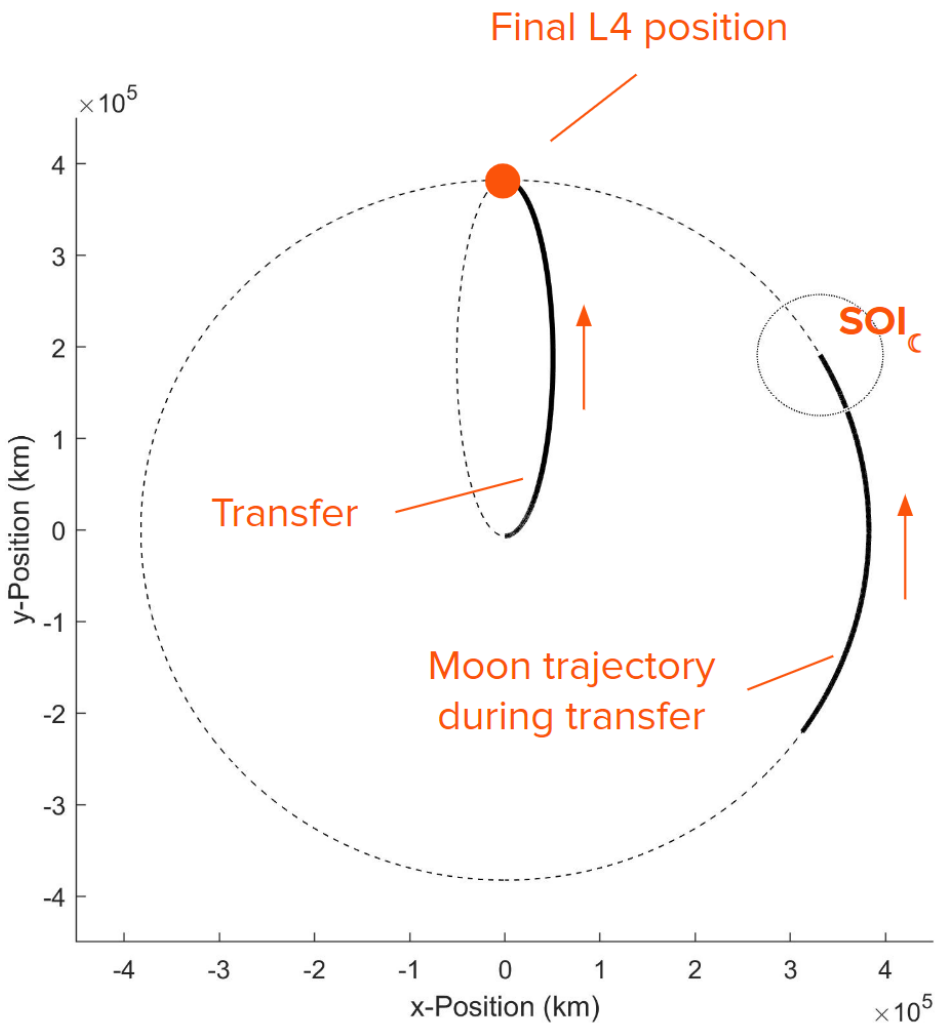

Figure 4: ECI transfer trajectory simulation including moon path and SOI

6.2 Multiple Shooting Method

The premise of the multiple shooting method is to solve for initial conditions, compare against a nominal path, compute the error, correct the error, and iterate until the error is negligible. The first step is to define the error which requires a reference as an ideal solution. We can define the nominal trajectory with the following state, $\vec{x}_n(\tau)$:

$$\vec{x}_n(\tau) = \begin{bmatrix} x_n(\tau) & y_n(\tau) & z_n(\tau) & \dot{x}_n(\tau) & \dot{y}_n(\tau) & \dot{z}_n(\tau) \end{bmatrix}^T$$

The difference from the nominal solution as a function of time, τ, can then be defined by $\delta\vec{x}(\tau)$ shown in Equation 8.

$$\delta\vec{x}(\tau) = \vec{x}(\tau) - \vec{x}_n(\tau) \tag{7}$$

The state space for the deviation from nominal state is then defined in Equation 8 with $A(\tau)$ being the state transition matrix defined in Equation 9. For this matrix, the potential energy partials are evaluated at the nominal solution; while the derivation of this matrix is not included in this paper, it is fairly simple to obtain when the equations of motion are written in terms of the potential energy at a given state.

$$\delta\dot{\vec{x}}(\tau) = A(\tau)\delta\vec{x}(\tau) \tag{8}$$

$$A(\tau) = \begin{bmatrix} 0 & 0 & 0 & 1 & 0 & 0 \\ 0 & 0 & 0 & 0 & 1 & 0 \\ 0 & 0 & 0 & 0 & 0 & 1 \\ U_{xx}|_{\vec{x}_n(\tau)} & U_{xy}|_{\vec{x}_n(\tau)} & U_{xz}|_{\vec{x}_n(\tau)} & 0 & 2 & 0 \\ U_{yx}|_{\vec{x}_n(\tau)} & U_{yy}|_{\vec{x}_n(\tau)} & U_{yz}|_{\vec{x}_n(\tau)} & -2 & 0 & 0 \\ U_{zx}|_{\vec{x}_n(\tau)} & U_{zy}|_{\vec{x}_n(\tau)} & U_{zz}|_{\vec{x}_n(\tau)} & 0 & 0 & 0 \end{bmatrix} \tag{9}$$

The relationship between one state at some initial time, τ_0, and some later time, τ, is then defined by the 6×6 matrix, $\Phi(\tau, \tau_0)$, in Equation 10. It's relationship with the state transition matrix then becomes the differential equation in Equation 11.

$$\Phi(\tau, \tau_0) = \frac{\delta\vec{x}(\tau)}{\delta\vec{x}(\tau_0)} \tag{10}$$

$$\dot{\Phi}(\tau, \tau_0) = A(\tau)\Phi(\tau, \tau_0) \tag{11}$$

The properties described above are useful when there is some desired state for some time, τ_f, often described as the final state. If the magnitude of τ_f is a design constraint, Equation 12 is useful in determining an initial state following this constraint, and converging to the nominal solution where the final state is known.

$$\delta\vec{x}(\tau_f) = \begin{bmatrix}\Phi(\tau_f, \tau_0) & \dot{\vec{x}}(\tau_f)\end{bmatrix} \begin{bmatrix}\delta\vec{x}(\tau_0) \\ \delta\tau_f\end{bmatrix} \tag{12}$$

In this problem, the final velocity is not a constraint on the trajectory design; when an L4 periodic orbit is reached, some Δv correction can be used to properly proceed to the next phase of the mission. Moreover, initial position may be known such that the only condition of interest to solve for a possible trajectory is the initial velocity. As such, we can define the error as the negative distance of the spacecraft from the final desired position where this deviation is defined below as $\delta\vec{r}(\tau)$. Evaluated at τ_f, error $\vec{e}$ is obtained per Equation 13.

$$\delta\vec{r}(\tau) = \begin{bmatrix}\delta x(\tau) & \delta y(\tau) & \delta z(\tau)\end{bmatrix}^T$$

$$\vec{e} = -\delta\vec{r}(\tau_f) \tag{13}$$

Based on this output error, a correction to the initial velocity guess is made via Equation 14. It is important to note that the 3×3 transition matrix in this expression comes directly from $\Phi(\tau, \tau_0)$ evaluated at τ_f; one can take the first three rows and last three columns of $\Phi(\tau_f, \tau_0)$. If τ_f is not known this process can also find the time required to reach the final state.

$$\begin{bmatrix}\delta\vec{v}(\tau_0) \\ \delta\tau_f\end{bmatrix} = \begin{bmatrix}\frac{\delta x(\tau_f)}{\delta\dot{x}(\tau_0)} & \frac{\delta x(\tau_f)}{\delta\dot{y}(\tau_0)} & \frac{\delta x(\tau_f)}{\delta\dot{z}(\tau_0)} & \dot{x}(\tau_f) \\ \frac{\delta y(\tau_f)}{\delta\dot{x}(\tau_0)} & \frac{\delta y(\tau_f)}{\delta\dot{y}(\tau_0)} & \frac{\delta y(\tau_f)}{\delta\dot{z}(\tau_0)} & \dot{y}(\tau_f) \\ \frac{\delta z(\tau_f)}{\delta\dot{x}(\tau_0)} & \frac{\delta z(\tau_f)}{\delta\dot{y}(\tau_0)} & \frac{\delta z(\tau_f)}{\delta\dot{z}(\tau_0)} & \dot{z}(\tau_f)\end{bmatrix}^+ \vec{e} \tag{14}$$

This method is iterated until the error vector is sufficiently small such that the initial velocity gets the spacecraft to the desired final state, $\vec{x}_n(\tau_f)$, with some defined tolerable deviation.

```
clear all; close all; clc;

m2 = 7.347673 * 10^(22);     % Mass of Moon (kg)
m1 = 5.97219 * 10^(24);      % Mass of Earth (kg)
mu = m2 / (m2 + m1);         % Earth-Moon Mass Ratio

r12 = 3.825 * 10^(5);        % Earth-Moon Distance (km)

C = 2.98799707128764;        % L4 Jacobi Constant


%% Calculations

% Short / Long Period about L4

s1 = 0.29820789544347032;
s2 = 0.95450094347526815;

dyn_short = dynICs_short(384.388174,0);
tau_short = 0:0.001:2*pi/s2;
x0 = [384.388174;
      0;
      -dyn_short(1);
      dyn_short(2)];
out_short = short(tau_short,x0);

dyn_long = dynICs_long(384.388174,0);
tau_long = 0:0.001:2*pi/s1;
x0 = [384.388174;
      0;
      -dyn_long(1);
      dyn_long(2)];
out_long = long(tau_long,x0);

% L4 ZVC
x1 = -mu;
x2 = 1 - mu;

[X,Y] = meshgrid(0.475:0.00001:0.5,0.855:0.00001:0.875);
Z = X.^2 + Y.^2 + 2.*(1-mu)./sqrt((X-x1).^2+Y.^2)...
    + 2.*mu./sqrt((X-x2).^2+Y.^2);



% Transfer
SOI_earth = 924000;      % km
SOI_moon = 66100;        % km
center_earth = [0 0];
center_moon = [r12 0];
moon_orb = 382500;
```

```
moon_rad = 1740;
earth_rad = 6378;

r0 = [1/2;sqrt(3)/2;0]*r12;
intercept = r0 + [384.388174;0;0];
r_int = norm(intercept);

G = 6.674 * 10^(-20); % km^3/kg-s^2
m1 = 5.97219 * 10^(24); % kg
mu = G * m1;

rp = 6678; % LEO
ra = r_int;

a = (rp+ra)/2;
e = 1 - rp/a;
p = a*(1 - e^2);
P = 2*pi*sqrt(a^3/mu);
P_half = P/2;
P_moon = 27.32*24*60^2;
n_frac_rad = 2*pi*P_half/P_moon;  % rad
n_frac_deg = n_frac_rad*180/pi;   % degrees

t = [];
x_sc = [];
y_sc = [];
x_moon = [];
y_moon = [];
f_sc = 0:0.001:pi;
f_moon = pi-n_frac_rad-pi/3:0.0003622:pi-pi/3;
for i = 1:length(f_sc)
    r_sc = p/(1+e*cos(f_sc(i)));
    x_sc(i) = r_sc*cos(f_sc(i));
    y_sc(i) = r_sc*sin(f_sc(i));
end
for i = 1:length(f_moon)
    x_moon(i) = r12*cos(f_moon(i));
    y_moon(i) = r12*sin(f_moon(i));
end

x_sc_full = [];
y_sc_full = [];
x_moon_full = [];
y_moon_full = [];
f = 0:0.0001:2*pi;
for i = 1:length(f)
    r_sc = p/(1+e*cos(f(i)));
    x_sc_full(i) = r_sc*cos(f(i));
    y_sc_full(i) = r_sc*sin(f(i));
```

```
    x_moon_full(i) = r12*cos(f(i));
    y_moon_full(i) = r12*sin(f(i));
end


%% Simulation

tspan = [0 105];
% x0 = [0.492506;0.85;0;0;0;0];
% x0 = [-5;5;0;-2;2;0];
x0 = [0;0.00008;0;0;0;0];
[~,dr] = ode89(@p9,tspan,x0);

% figure(1)
% plot(dr(:,1),dr(:,2))
% xlabel('x-Position (non-dim)')
% ylabel('y-Position (non-dim)')
%
% figure(2)
% hold on
% plot(out_long(1,:),out_long(2,:))
% plot(out_short(1,:),out_short(2,:))
% legend('Long Period (s_1)','Short Period (s_2)')
% xlim([-900 900])
% ylim([-700 700])
% xlabel('x-Position (km)')
% ylabel('y-Position (km)')
%
% figure(3)
% hold on
% plot(dr(:,1),dr(:,2),'r--')
% plot(out_short(1,:)/r12,out_short(2,:)/r12,'m')
% plot(out_long(1,:)/r12,out_long(2,:)/r12,'b')
% xlim([-900 900]/r12)
% ylim([-700 700]/r12)

figure(4)
contourf(X,Y,2*C-Z,[C C])
xlim([0.475 0.5])
ylim([0.855 0.875])
xlabel('x-Position')
ylabel('y-Position')
title('Zero Velocity Surface for L4')

% figure(5)
% hold on
% viscircles(center_earth,SOI_earth,'Color','k','LineStyle',':','LineWidth',0.5);
% viscircles(center_moon,SOI_moon,'Color','k','LineStyle',':','LineWidth',0.5);
% viscircles(center_earth,moon_orb,'Color','k','LineStyle','--','LineWidth',0.75);
% viscircles(center_earth,earth_rad,'Color','k');
```

```
% viscircles(center_moon,moon_rad,'Color','k');
% xlim([-1.2e6 1.2e6])
% ylim([-1.2e6 1.2e6])

figure(6)
hold on
plot(y_sc,-x_sc,'Color','k','LineWidth',2)
plot(y_moon,-x_moon,'Color','k','LineWidth',2)
plot(y_sc_full,-x_sc_full,'k--')
plot(y_moon_full,-x_moon_full,'k--')
viscircles([y_moon(end) -x_moon(end)],SOI_moon,'Color','k','LineStyle',':','LineWidth',↙
0.5);
xlim([-4.5e5 4.5e5])
ylim([-4.5e5 4.5e5])
xlabel('x-Position (km)')
ylabel('y-Position (km)')



%% Functions

function dyn = dynICs_short(zeta0,eta0)

m2 = 7.347673 * 10^(22);     % Mass of Moon (kg)
m1 = 5.97219 * 10^(24);      % Mass of Earth (kg)
mu = m2 / (m2 + m1);         % Earth-Moon Mass Ratio

% s1 = 0.29820789544347032;
s2 = 0.95450094347526815;

Uxx = 3/4;
Uxy = 3*sqrt(3)/2 * (mu-1/2);

Gamma = (s2^2 + Uxx) / (4*s2^2 + Uxy^2);

zeta0dot = 1/2 * (Uxy*zeta0 + eta0/Gamma);
eta0dot = -1/2 * ((s2^2 + Uxx)*zeta0 + Uxy*eta0);

dyn = [zeta0dot;eta0dot];

end

function dyn = dynICs_long(zeta0,eta0)

m2 = 7.347673 * 10^(22);     % Mass of Moon (kg)
m1 = 5.97219 * 10^(24);      % Mass of Earth (kg)
mu = m2 / (m2 + m1);         % Earth-Moon Mass Ratio

s1 = 0.29820789544347032;
% s2 = 0.95450094347526815;
```

```
Uxx = 3/4;
Uxy = 3*sqrt(3)/2 * (mu-1/2);

Gamma = (s1^2 + Uxx) / (4*s1^2 + Uxy^2);

zeta0dot = 1/2 * (Uxy*zeta0 + eta0/Gamma);
eta0dot = -1/2 * ((s1^2 + Uxx)*zeta0 + Uxy*eta0);

dyn = [zeta0dot;eta0dot];

end

function state = short(tau,in)

% s1 = 0.29820789544347032;
s2 = 0.95450094347526815;

zeta0 = in(1);
eta0 = in(2);
zeta0dot = in(3);
eta0dot = in(4);

zeta = [];
eta = [];
for i = 1:length(tau)
    zeta(i) = zeta0*cos(s2*tau(i)) + zeta0dot/s2*sin(s2*tau(i));
    eta(i) = eta0*cos(s2*tau(i)) + eta0dot/s2*sin(s2*tau(i));
end

state = [zeta;eta];

end

function state = long(tau,in)

s1 = 0.29820789544347032;
% s2 = 0.95450094347526815;

zeta0 = in(1);
eta0 = in(2);
zeta0dot = in(3);
eta0dot = in(4);

zeta = [];
eta = [];
for i = 1:length(tau)
    zeta(i) = zeta0*cos(s1*tau(i)) + zeta0dot/s1*sin(s1*tau(i));
    eta(i) = eta0*cos(s1*tau(i)) + eta0dot/s1*sin(s1*tau(i));
end
```

```
state = [zeta;eta];

end

function dr_dt = p9(~,in)

m2 = 7.347673 * 10^(22);     % Mass of Moon (kg)
m1 = 5.97219 * 10^(24);      % Mass of Earth (kg)
mu = m2 / (m2 + m1);         % Earth-Moon Mass Ratio

dr = [in(1);in(2);in(3)];
dr_dot = [in(4);in(5);in(6)];

Omega = [0;0;1];
Otilde = [0 -Omega(3) Omega(2);Omega(3) 0 -Omega(1);-Omega(2) Omega(1) 0];

F = (1-mu)/4 * [-1 3*sqrt(3) 0;3*sqrt(3) 5 0;0 0 -4] + ...
    mu/4 * [-1 -3*sqrt(3) 0;-3*sqrt(3) 5 0;0 0 -4];

M = [zeros(3) eye(3);F-Otilde^2 -2*Otilde];
dr_dt = M * [dr;dr_dot];

end
```